Amplitude-Based Analyses at GlueX

Boris Grube*

on behalf of the GlueX Collaboration

*Thomas Jefferson National Accelerator Facility

Workshop on AI for Hadron Spectroscopy at JLab

June 4, 2025

Jefferson Lab, Newport News, VA

Meson spectroscopy and photoproduction

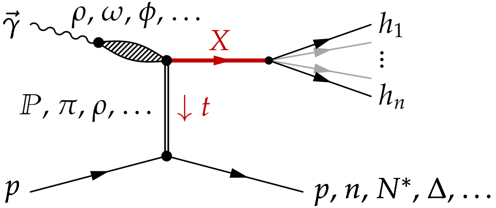

Rich process

- Light mesons with all J^{PC} quantum numbers accessible in various decay modes
- Produced by various exchange processes
- Linear beam polarization helps to disentangle production mechanisms
- Provides mostly complementary information to existing data

Goal: precision measurement of light-meson spectrum

- Confirm higher excited conventional states
- Complete $\mathrm{SU(3)}_{\mathrm{flavor}}$ multiplets
- Search for exotic states beyond $q\bar{q}$

Meson spectroscopy and photoproduction

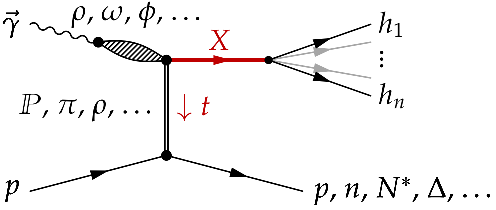

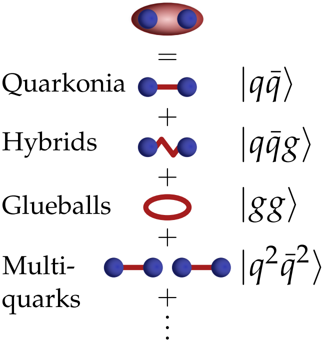

Rich process

- Light mesons with all J^{PC} quantum numbers accessible in various decay modes
- Produced by various exchange processes
- Linear beam polarization helps to disentangle production mechanisms
- Provides mostly complementary information to existing data

Goal: precision measurement of light-meson spectrum

- Confirm higher excited conventional states
- Complete $\text{SU(3)}_{\text{flavor}}$ multiplets
- Search for exotic states beyond $q\bar{q}$

Best exotic light-meson candidate: $\pi_1(1600)$

Spin-exotic $J^{PC} = 1^{-+}$ quantum numbers

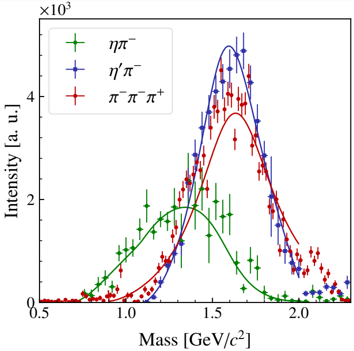

- Best evidence in COMPASS $\eta\pi$, $\eta'\pi$, and $\rho(770)\pi$ data from pion diffraction

  COMPASS, PLB **740** (2015) 303; PRD **105** (2022) 1012005; PRD **98** (2018) 092003; PRL **104** (2010) 241803

- JPAC coupled-channel analysis: $\eta\pi$ and $\eta'\pi$ data can be described by single resonance pole consistent with $\pi_1(1600)$

  Rodas *et al.* [JPAC], PRL **122** (2019) 042002

- Recent find by BESIII: isoscalar partner $\eta_1(1855)$

  BESIII, PRL **129** (2022) 192002

Best exotic light-meson candidate: $\pi_1(1600)$

Spin-exotic $J^{PC} = 1^{-+}$ quantum numbers

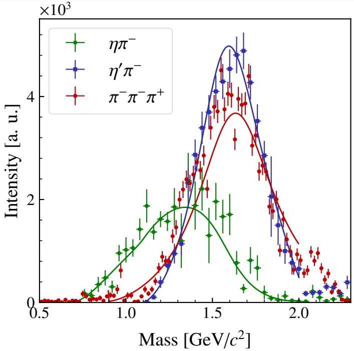

JPAC analysis of $\eta^{(\prime)}\pi$ COMPASS data

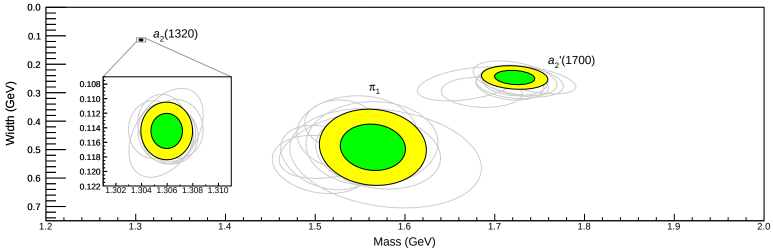

- Best evidence in COMPASS $\eta\pi$, $\eta'\pi$, and $\rho(770)\pi$ data from pion diffraction

  COMPASS, PLB **740** (2015) 303; PRD **105** (2022) 1012005; PRD **98** (2018) 092003; PRL **104** (2010) 241803

- JPAC coupled-channel analysis: $\eta\pi$ and $\eta'\pi$ data can be described by single resonance pole consistent with $\pi_1(1600)$

  Rodas *et al.* [JPAC], PRL **122** (2019) 042002

- Recent find by BESIII: isoscalar partner $\eta_1(1855)$

  BESIII, PRL **129** (2022) 192002

Best exotic light-meson candidate: $\pi_1(1600)$

Spin-exotic $J^{PC} = 1^{-+}$ quantum numbers

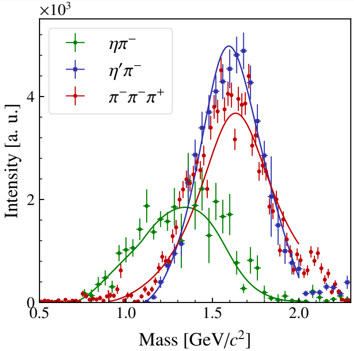

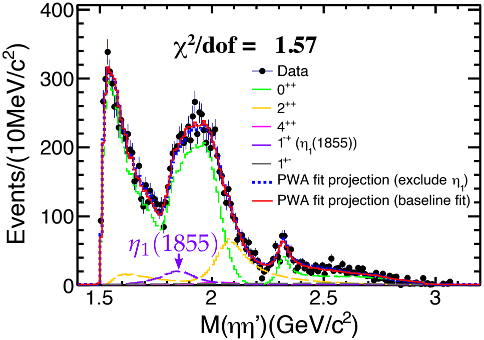

- Best evidence in COMPASS $\eta\pi$, $\eta'\pi$, and $\rho(770)\pi$ data from pion diffraction

  COMPASS, PLB **740** (2015) 303; PRD **105** (2022) 1012005; PRD **98** (2018) 092003; PRL **104** (2010) 241803
- JPAC coupled-channel analysis: $\eta\pi$ and $\eta'\pi$ data can be described by single resonance pole consistent with $\pi_1(1600)$

  Rodas *et al.* [JPAC], PRL **122** (2019) 042002
- Recent find by BESIII: isoscalar partner $\eta_1(1855)$

  BESIII, PRL **129** (2022) 192002

Searching for exotic mesons at GlueX

Jefferson Lab
Thomas Jefferson National Accelerator Facility

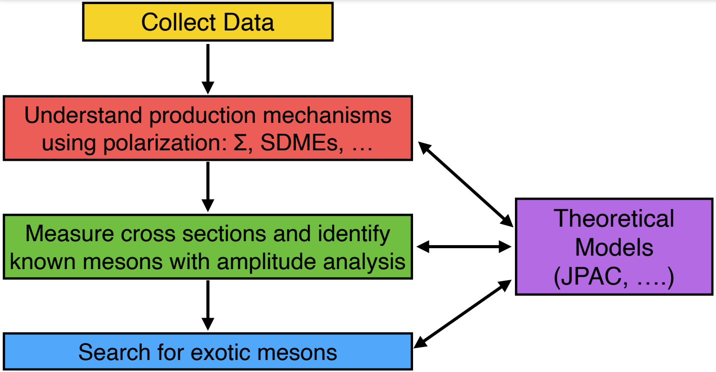

- Amplitude analysis essential to extract meson spectrum
- *Strategy:* understand photoproduction of well-known states first and then use them as reference when searching for exotic states
- “Golden channels” for π_1 search: $\eta\pi$ and $\eta'\pi$

This talk: focus on common challenges encountered in amplitude analyses

- Improving stability of fit results by imposing continuity constraints on amplitudes
- How to take into account non-resonant contributions?
- Moment analysis as an additional avenue

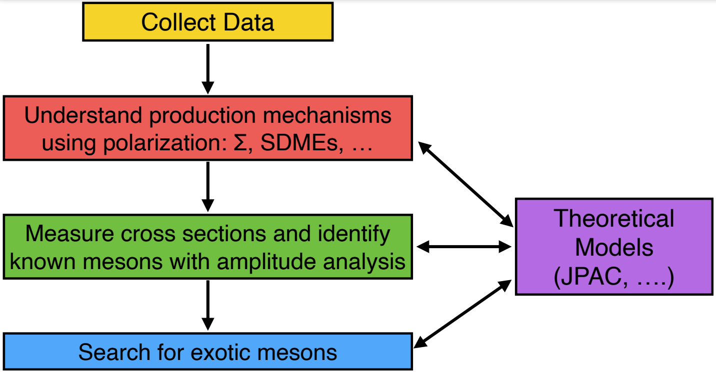

- Amplitude analysis essential to extract meson spectrum
- *Strategy:* understand photoproduction of well-known states first and then use them as reference when searching for exotic states
- "Golden channels" for π_1 search: $\eta\pi$ and $\eta'\pi$

This talk: focus on common challenges encountered in amplitude analyses

- Improving stability of fit results by imposing continuity constraints on amplitudes
- How to take into account non-resonant contributions?
- Moment analysis as an additional avenue

Searching for exotic mesons at GlueX

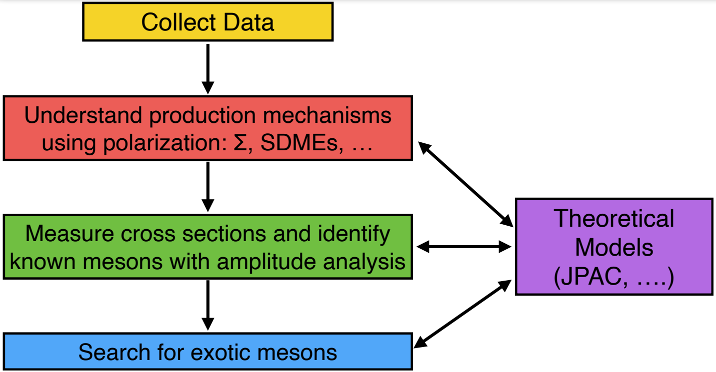

- Amplitude analysis essential to extract meson spectrum
- *Strategy:* understand photoproduction of well-known states first and then use them as reference when searching for exotic states
- "Golden channels" for π_1 search: $\eta\pi$ and $\eta'\pi$

This talk: focus on common challenges encountered in amplitude analyses

- Improving stability of fit results by imposing continuity constraints on amplitudes
- How to take into account non-resonant contributions?
- Moment analysis as an additional avenue

Why $\eta^{(\prime)}\pi$?

- Experimentally clean channels
- Two-body final states are easiest to model
- All waves with odd orbital angular momentum are spin-exotic, e.g. P-wave has $J^{PC} = 1^{-+}$
- Use well known $a_2(1320)$ as reference
- Multiple $\eta^{(\prime)}$ decay modes accessible, e.g. $\eta \to \gamma\gamma$ and $\pi^+\pi^-\pi^0$
  - Assess systematics from acceptance and backgrounds
- Test our understanding of production mechanisms:
  - Linear polarization of beam photons $\Longrightarrow$ separation of natural- and unnatural-parity exchange
  - Multiple production channels accessible, e.g.
    - $\gamma\, p \to \eta\pi^0\, p$: mostly ρ and ω exchange
    - $\gamma\, p \to \eta\pi^-\, \Delta^{++}$: mostly π exchange

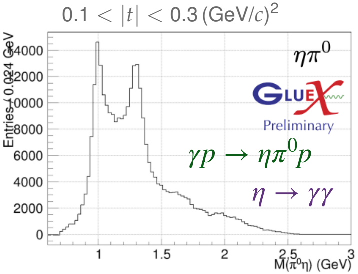

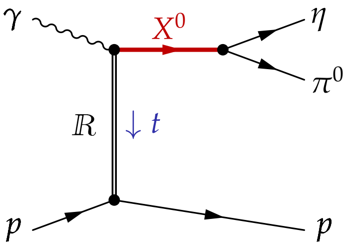

- Experimentally clean channels
- Two-body final states are easiest to model
- All waves with odd orbital angular momentum are spin-exotic, e.g. P-wave has $J^{PC} = 1^{-+}$
- Use well known $a_2(1320)$ as reference
- Multiple $\eta^{(\prime)}$ decay modes accessible, e.g. $\eta \to \gamma\gamma$ and $\pi^+\pi^-\pi^0$
    - Assess systematics from acceptance and backgrounds
- Test our understanding of production mechanisms:
    - Linear polarization of beam photons $\Longrightarrow$ separation of natural- and unnatural-parity exchange
    - Multiple production channels accessible, e.g.
        - $\gamma\, p \to \eta\pi^0\, p$: mostly ρ and ω exchange
        - $\gamma\, p \to \eta\pi^-\, \Delta^{++}$: mostly π exchange

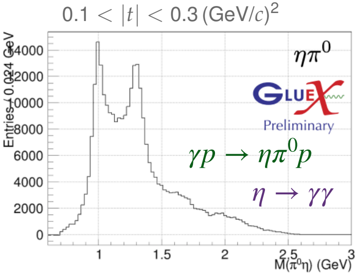

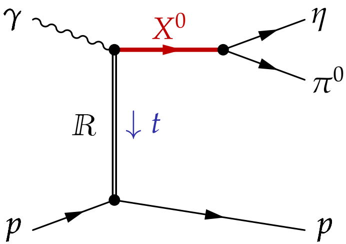

- Experimentally clean channels
- Two-body final states are easiest to model
- All waves with odd orbital angular momentum are spin-exotic, e.g. P-wave has $J^{PC} = 1^{-+}$
- Use well known $a_2(1320)$ as reference
- Multiple $\eta^{(\prime)}$ decay modes accessible, e.g. $\eta \to \gamma\gamma$ and $\pi^+\pi^-\pi^0$
  - Assess systematics from acceptance and backgrounds
- Test our understanding of production mechanisms:
  - Linear polarization of beam photons $\Longrightarrow$ separation of natural- and unnatural-parity exchange
  - Multiple production channels accessible, e.g.
    - $\gamma\, p \to \eta\pi^0\, p$: mostly ρ and ω exchange
    - $\gamma\, p \to \eta\pi^-\, \Delta^{++}$: mostly π exchange

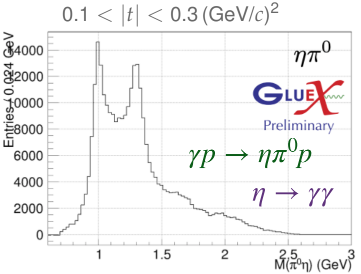

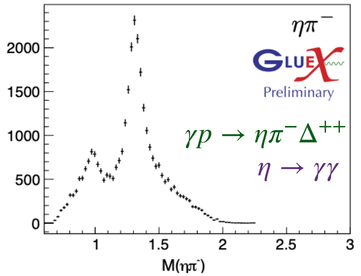

$\gamma\, p \to \eta\pi^0\, p$ and $\gamma\, p \to \eta\pi^-\, \Delta^{++}$; $\eta \to \gamma\gamma$

Non-trivial dependence on 4-momentum transfer

Jefferson Lab
Thomas Jefferson National Accelerator Facility

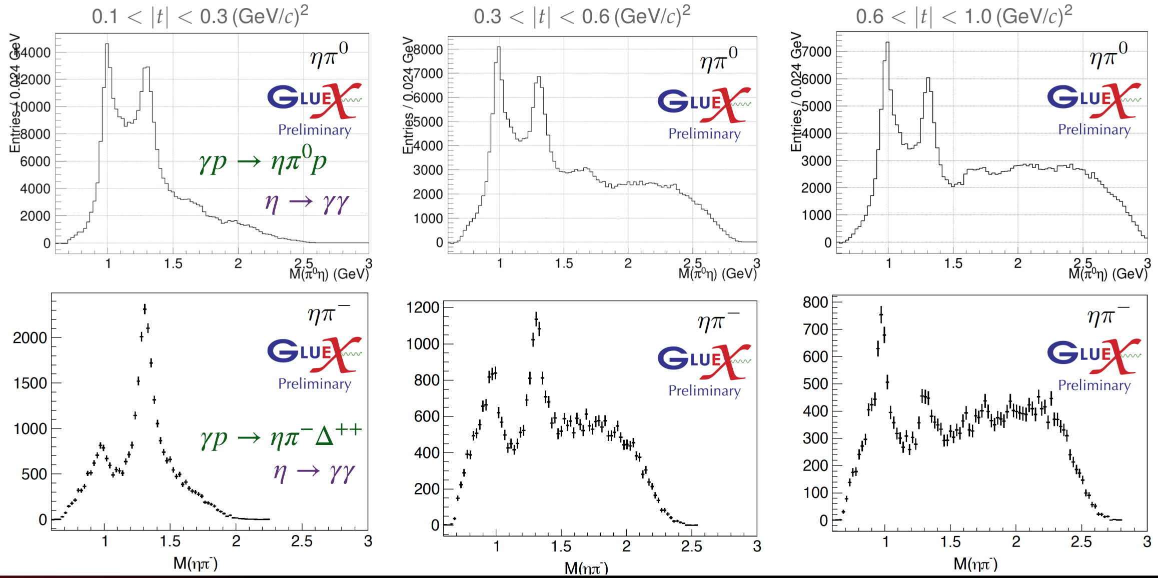

PWA model for linearly polarized photon beam

Mathieu *et al.* [JPAC], PRD **100** (2019) 054017

- **3 Angles:**
  - $\Omega = (\theta, \phi)$ angles of η in $\eta\pi$ rest frame
  - Φ is angle between γ polarization vector and production plane
- Linear beam polarization P_γ distinguishes between naturality $(\pm)$ of exchange ($=$ reflectivity)

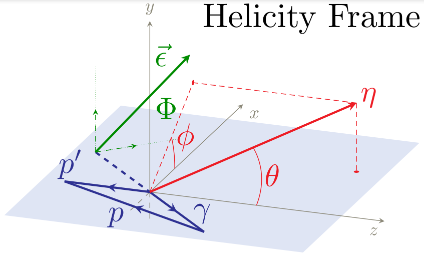

- **Intensity model** with angular amplitude $Z_\ell^m(\Omega, \Phi) \equiv Y_\ell^m(\Omega)\, e^{-i\Phi}$

$$
\begin{aligned}
\mathcal{I}(\Omega, \Phi) \propto (1 - P_\gamma) \left| \sum_{\ell,m} [\ell]_m^{(-)} \operatorname{Re}\left[Z_\ell^m(\Omega, \Phi)\right] \right|^2 + (1 - P_\gamma) \left| \sum_{\ell,m} [\ell]_m^{(+)} \operatorname{Im}\left[Z_\ell^m(\Omega, \Phi)\right] \right|^2 \\
+ (1 + P_\gamma) \left| \sum_{\ell,m} [\ell]_m^{(+)} \operatorname{Re}\left[Z_\ell^m(\Omega, \Phi)\right] \right|^2 + (1 + P_\gamma) \left| \sum_{\ell,m} [\ell]_m^{(-)} \operatorname{Im}\left[Z_\ell^m(\Omega, \Phi)\right] \right|^2
\end{aligned}
$$

- Wave set grows quickly with ℓ: $S_0^\pm$, $P_{-1,0,+1}^\pm$, $D_{-2,-1,0,+1,+2}^\pm$, $\cdots$

PWA model for linearly polarized photon beam

Mathieu *et al.* [JPAC], PRD **100** (2019) 054017

- **3 Angles:**
  - $\Omega = (\theta, \phi)$ angles of η in $\eta\pi$ rest frame
  - Φ is angle between γ polarization vector and production plane
- Linear beam polarization P_γ distinguishes between naturality $(\pm)$ of exchange (= reflectivity)

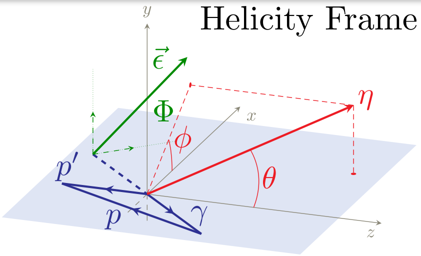

- **Intensity model** with angular amplitude $Z_\ell^m(\Omega, \Phi) \equiv Y_\ell^m(\Omega)\, e^{-i\Phi}$

$$\mathcal{I}(\Omega,\Phi) \propto (1 - P_\gamma) \left| \sum_{\ell,m} [\ell]_m^{(-)} \operatorname{Re}\left[Z_\ell^m(\Omega,\Phi)\right] \right|^2 + (1 - P_\gamma) \left| \sum_{\ell,m} [\ell]_m^{(+)} \operatorname{Im}\left[Z_\ell^m(\Omega,\Phi)\right] \right|^2$$

$$+ (1 + P_\gamma) \left| \sum_{\ell,m} [\ell]_m^{(+)} \operatorname{Re}\left[Z_\ell^m(\Omega,\Phi)\right] \right|^2 + (1 + P_\gamma) \left| \sum_{\ell,m} [\ell]_m^{(-)} \operatorname{Im}\left[Z_\ell^m(\Omega,\Phi)\right] \right|^2$$

- Wave set grows quickly with ℓ: $S_0^\pm$, $P_{-1,0,+1}^\pm$, $D_{-2,-1,0,+1,+2}^\pm$, $\cdots$

PWA model for linearly polarized photon beam

Mathieu *et al.* [JPAC], PRD **100** (2019) 054017

- **3 Angles:**
  - $\Omega = (\theta, \phi)$ angles of η in $\eta\pi$ rest frame
  - Φ is angle between γ polarization vector and production plane
- Linear beam polarization P_γ distinguishes between naturality $(\pm)$ of exchange $(=$ reflectivity)

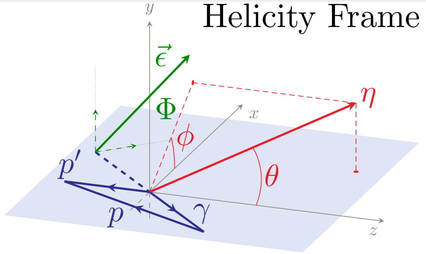

- **Intensity model** with angular amplitude $Z_\ell^m(\Omega, \Phi) \equiv Y_\ell^m(\Omega)\, e^{-i\Phi}$

$$\mathcal{I}(\Omega, \Phi) \propto (1 - P_\gamma) \left| \sum_{\ell,m} [\ell]_m^{(-)} \operatorname{Re}\left[Z_\ell^m(\Omega, \Phi)\right] \right|^2 + (1 - P_\gamma) \left| \sum_{\ell,m} [\ell]_m^{(+)} \operatorname{Im}\left[Z_\ell^m(\Omega, \Phi)\right] \right|^2$$

$$+ (1 + P_\gamma) \left| \sum_{\ell,m} [\ell]_m^{(+)} \operatorname{Re}\left[Z_\ell^m(\Omega, \Phi)\right] \right|^2 + (1 + P_\gamma) \left| \sum_{\ell,m} [\ell]_m^{(-)} \operatorname{Im}\left[Z_\ell^m(\Omega, \Phi)\right] \right|^2$$

- Wave set grows quickly with ℓ: $S_0^\pm, P_{-1,0,+1}^\pm, D_{-2,-1,0,+1,+2}^\pm, \cdots$

PWA model for linearly polarized photon beam

Mathieu *et al.* [JPAC], PRD **100** (2019) 054017

- **3 Angles:**
  - $\Omega = (\theta, \phi)$ angles of η in $\eta\pi$ rest frame
  - Φ is angle between γ polarization vector and production plane
- Linear beam polarization P_γ distinguishes between naturality $(\pm)$ of exchange $(=$ reflectivity)

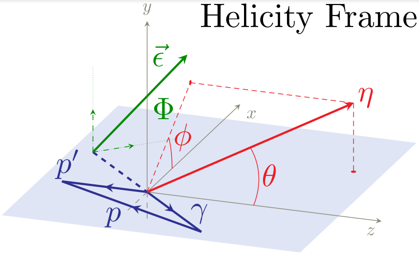

- **Intensity model** with angular amplitude $Z_\ell^m(\Omega, \Phi) \equiv Y_\ell^m(\Omega)\, e^{-i\Phi}$

$$\mathcal{I}(\Omega, \Phi) \propto (1 - P_\gamma) \left| \sum_{\ell,m} [\ell]_m^{(-)} \operatorname{Re}\left[Z_\ell^m(\Omega, \Phi)\right] \right|^2 + (1 - P_\gamma) \left| \sum_{\ell,m} [\ell]_m^{(+)} \operatorname{Im}\left[Z_\ell^m(\Omega, \Phi)\right] \right|^2$$

$$+ (1 + P_\gamma) \left| \sum_{\ell,m} [\ell]_m^{(+)} \operatorname{Re}\left[Z_\ell^m(\Omega, \Phi)\right] \right|^2 + (1 + P_\gamma) \left| \sum_{\ell,m} [\ell]_m^{(-)} \operatorname{Im}\left[Z_\ell^m(\Omega, \Phi)\right] \right|^2$$

- Wave set grows quickly with ℓ: $S_0^\pm$, $P_{-1,0,+1}^\pm$, $D_{-2,-1,0,+1,+2}^\pm$, $\cdots$

Mass-independent PWA of $\gamma\, p \to \eta\pi^0\, p;\, \eta \to \gamma\gamma$

Low $|t|$: 0.1 $< |t| <$ 0.3 (GeV/c)^2

- Waveset based on tensor-meson dominance (TMD) model: $\{S_0^{\pm}, D_{-1}^{-}, D_0^{\pm}, D_{+1}^{\pm}, D_{+2}^{+}\}$

  Mathieu *et al.* [JPAC], PRD **102** (2020) 014003

- Mostly natural exchange
- Sizable S_0^{+}-wave contribution
  - $a_0(980)$ and $a_0(1450)$ signals?
  - Leakage from $a_2(1320)$?
  - Non-resonant contributions?
- Clear $a_2(1320)$ signal with $m = +2$ in natural exchange ($=$ positive reflectivity)
- *Challenges:*
  - Model selection: what is the optimal wave set?
  - Large bin-to-bin fluctuations of partial-wave amplitudes of some waves

Mass-independent PWA of $\gamma\, p \to \eta\pi^0\, p;\ \eta \to \gamma\gamma$

Low $|t|$: $0.1 < |t| < 0.3\,(\mathrm{GeV}/c)^2$

- Waveset based on tensor-meson dominance (TMD) model: $\{S_0^\pm, D_{-1}^-, D_0^\pm, D_{+1}^\pm, D_{+2}^+\}$

  Mathieu *et al.* [JPAC], PRD **102** (2020) 014003

- Mostly natural exchange
- Sizable S_0^+-wave contribution
  - $a_0(980)$ and $a_0(1450)$ signals?
  - Leakage from $a_2(1320)$?
  - Non-resonant contributions?
- Clear $a_2(1320)$ signal with $m = +2$ in natural exchange (= positive reflectivity)
- *Challenges:*
  - Model selection: what is the optimal wave set?
  - Large bin-to-bin fluctuations of partial-wave amplitudes of some waves

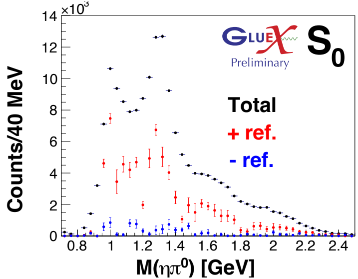

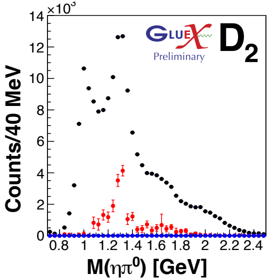

Mass-independent PWA of $\gamma\, p \to \eta\pi^0\, p;\, \eta \to \gamma\gamma$

Low $|t|$: $0.1 < |t| < 0.3\,(\text{GeV}/c)^2$

- Waveset based on tensor-meson dominance (TMD) model: $\{S_0^\pm, D_{-1}^-, D_0^\pm, D_{+1}^\pm, D_{+2}^+\}$

  Mathieu *et al.* [JPAC], PRD **102** (2020) 014003
- Mostly natural exchange
- Sizable S_0^+-wave contribution
  - $a_0(980)$ and $a_0(1450)$ signals?
  - Leakage from $a_2(1320)$?
  - Non-resonant contributions?
- Clear $a_2(1320)$ signal with $m = +2$ in natural exchange ($=$ positive reflectivity)
- *Challenges:*
  - Model selection: what is the optimal wave set?
  - Large bin-to-bin fluctuations of partial-wave amplitudes of some waves

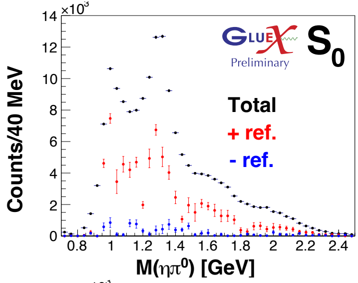

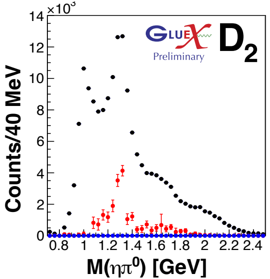

Interlude: two-pseudoscalar system

Ambiguities

- Spinless beam particle: mathematical ambiguities in form of Barrelet zeros

  Chung, PRD **56** (1997) 7299
- Photoproduction:
  - No Barrelet zeros — Smith *et al.* [JPAC], PRD **108** (2023) 076001
  - *Work in progress:* find continuous mathematical ambiguities for special wave sets
    - Probably not relevant for most analyses

Local minima of negative log-likelihood function

- Input-output studies
  - Generate events from intensity distribution with known amplitudes and assuming 35 % beam polarization
  - Assume ideal case: fit generated events, i.e. no detector effects, with true wave set
  - Perform 100 PWA fit attempts with random initial values of amplitudes using MINUIT MIGRAD

Ambiguities

- Spinless beam particle: mathematical ambiguities in form of Barrelet zeros

  Chung, PRD **56** (1997) 7299
- Photoproduction:
  - No Barrelet zeros — Smith *et al.* [JPAC], PRD **108** (2023) 076001
  - *Work in progress:* find continuous mathematical ambiguities for special wave sets
    - Probably not relevant for most analyses

Local minima of negative log-likelihood function

- Input-output studies
  - Generate events from intensity distribution with known amplitudes and assuming 35 % beam polarization
  - Assume ideal case: fit generated events, i.e. no detector effects, with true wave set
  - Perform 100 PWA fit attempts with random initial values of amplitudes using MINUIT MIGRAD

Interlude: two-pseudoscalar system

Local minima of negative log-likelihood function (NLL)

$\{S_0^{\pm}, P_{+1}^{\pm}, P_0^{\pm}, P_{-1}^{\pm}\}$ wave set, 10^6 events

Same wave set, 10^5 events

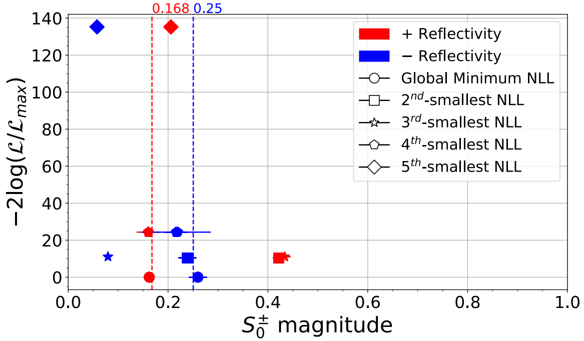

- Global minimum: estimated amplitudes consistent with input values
- Additional local minima close in likelihood
  - Amplitudes deviate significantly from input values

- Global minimum not consistent with input values
- First local minimum:
  - Only 0.5 units of log-likelihood worse
  - Consistent with input values

Interlude: two-pseudoscalar system

Local minima of negative log-likelihood function (NLL)

$\{S_0^{\pm}, P_{+1}^{\pm}, P_0^{\pm}, P_{-1}^{\pm}\}$ wave set, 10^6 events

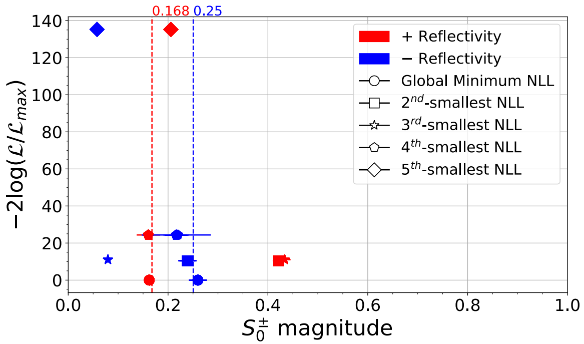

- Global minimum: estimated amplitudes consistent with input values
- Additional local minima close in likelihood
  - Amplitudes deviate significantly from input values

Same wave set, 10^5 events

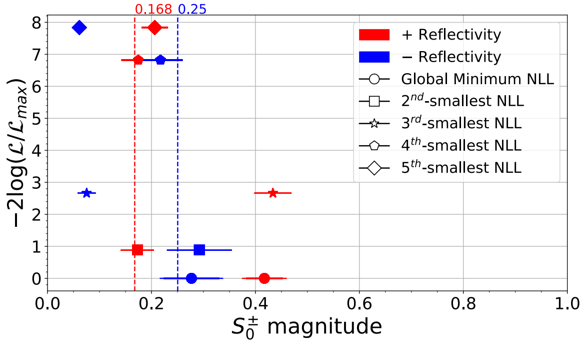

- Global minimum not consistent with input values
- First local minimum:
  - Only 0.5 units of log-likelihood worse
  - Consistent with input values

Interlude: two-pseudoscalar system

Local minima of negative log-likelihood function (NLL)

$\{S_0^{\pm}, P_{+1}^{\pm}, P_0^{\pm}, P_{-1}^{\pm}\}$ wave set, 10^6 events

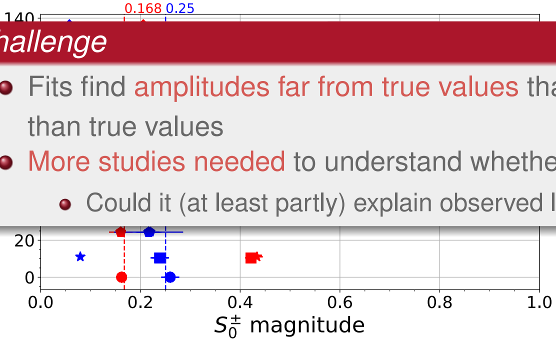

Same wave set, 10^5 events

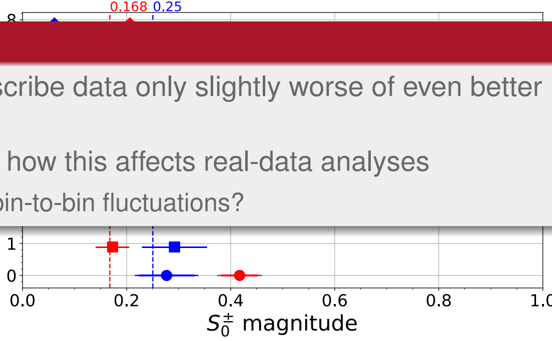

Challenge

- Fits find amplitudes far from true values that describe data only slightly worse of even better than true values
- More studies needed to understand whether and how this affects real-data analyses
  - Could it (at least partly) explain observed large bin-to-bin fluctuations?

- Global minimum: estimated amplitudes consistent with input values
- Additional local minima close in likelihood
  - Amplitudes deviate significantly from input values

- Global minimum not consistent with input values
- First local minimum:
  - Only 0.5 units of log-likelihood worse
  - Consistent with input values

- Constrain mass dependence of selected amplitudes:
  - Model D-waves using sum of $a_2(1320)$ and $a_2(1700)$ Breit-Wigner amplitudes
- Keep mass-independent parametrization for S-waves
- TMD wave set $\{S_0^{\pm}, D_{-1}^{-}, D_0^{\pm}, D_{+1}^{\pm}, D_{+2}^{+}\}$: notable deviations from data at large $-t$
- Include all allowed S- and D-waves in fit, i.e. $\{S_0^{\pm}, D_{+2,+1,0,-1,-2}^{\pm}\}$
- For given naturality: constrain production phases of all m states of a given a_2 resonance to be identical

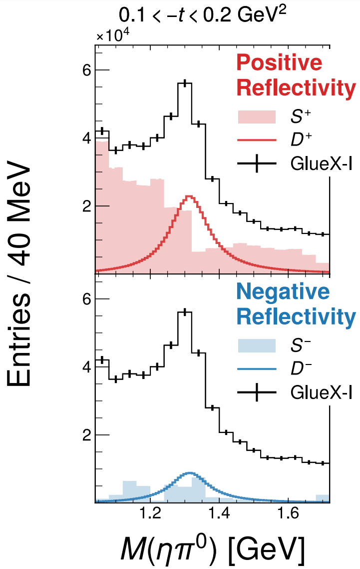

- Constrain mass dependence of selected amplitudes:
  - Model D-waves using sum of $a_2(1320)$ and $a_2(1700)$ Breit-Wigner amplitudes
- Keep mass-independent parametrization for S-waves
- TMD wave set $\{S_0^\pm, D_{-1}^-, D_0^\pm, D_{+1}^\pm, D_{+2}^+\}$: notable deviations from data at large $-t$
- Include all allowed S- and D-waves in fit, i.e. $\{S_0^\pm, D_{+2,+1,0,-1,-2}^\pm\}$
- For given naturality: constrain production phases of all m states of a given a_2 resonance to be identical

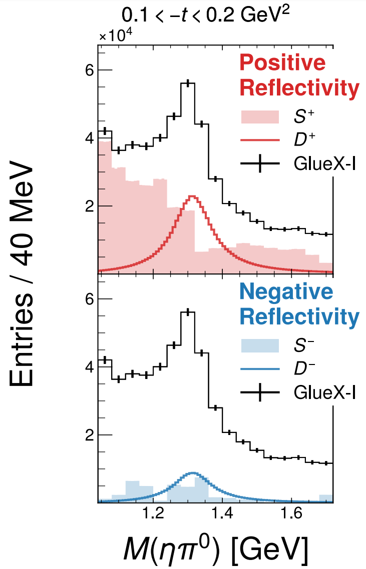

PWA of $\gamma\, p \to \eta\pi^0\, p;\, \eta \to \gamma\gamma$

Hybrid PWA approach

arXiv:2501.03091

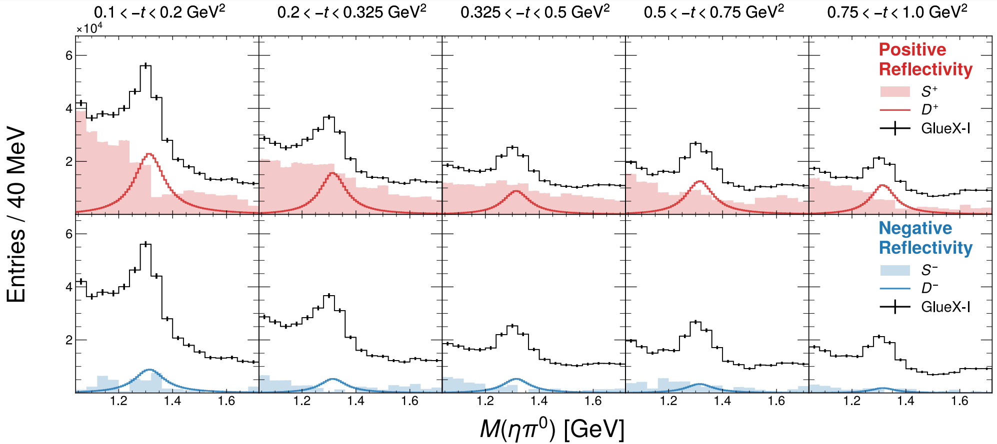

- Eliminates leakage between S- and D-waves
- Dominant contributions consistent with mass-independent PWA

$a_2(1320)$ differential cross section

arXiv:2501.03091

Jefferson Lab
Thomas Jefferson National Accelerator Facility

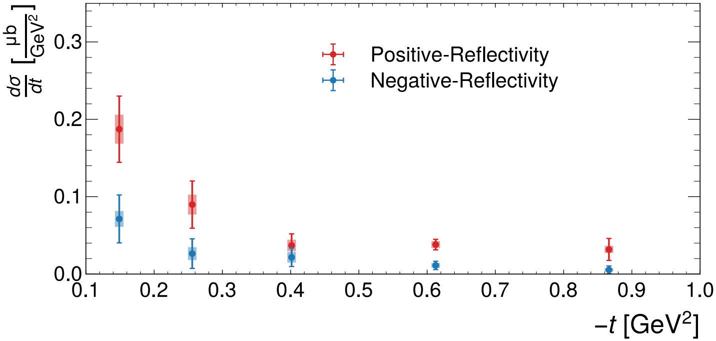

- First separation of contributions from natural and unnatural exchanges
  - Requires beam polarization; unique to GlueX
- Total cross section predicted by TMD model agrees well with data

Mathieu *et al.* [JPAC], PRD **102** (2020) 014003

$a_2(1320)$ differential cross section

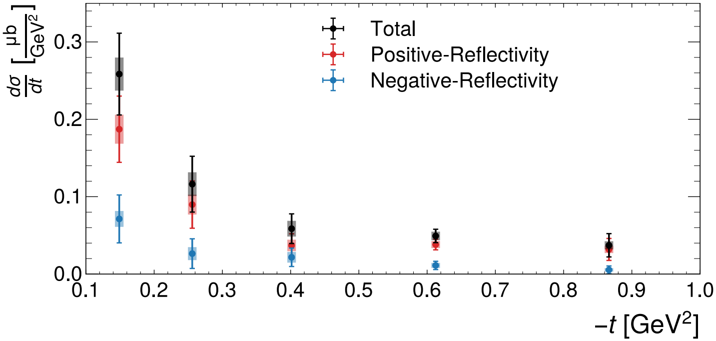

- First separation of contributions from natural and unnatural exchanges
  - Requires beam polarization; unique to GlueX
- Total cross section predicted by TMD model agrees well with data

Mathieu *et al.* [JPAC], PRD **102** (2020) 014003

$a_2(1320)$ differential cross section

arXiv:2501.03091

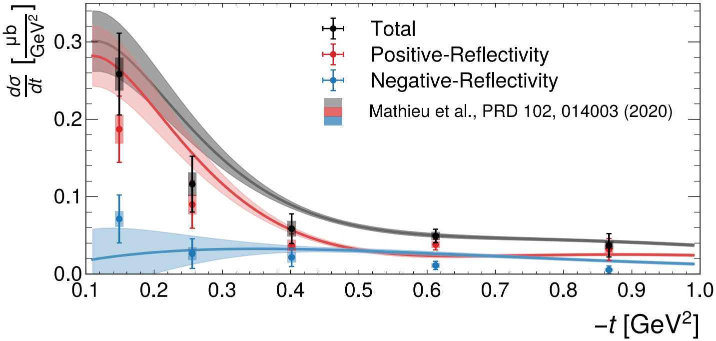

- First separation of contributions from natural and unnatural exchanges
  - Requires beam polarization; unique to GlueX
- Total cross section predicted by TMD model agrees well with data

Mathieu *et al.* [JPAC], PRD **102** (2020) 014003

$a_2(1320)$ parity asymmetry

$$P_\sigma = \frac{d\sigma^+/dt - d\sigma^-/dt}{d\sigma^+/dt + d\sigma^-/dt}$$

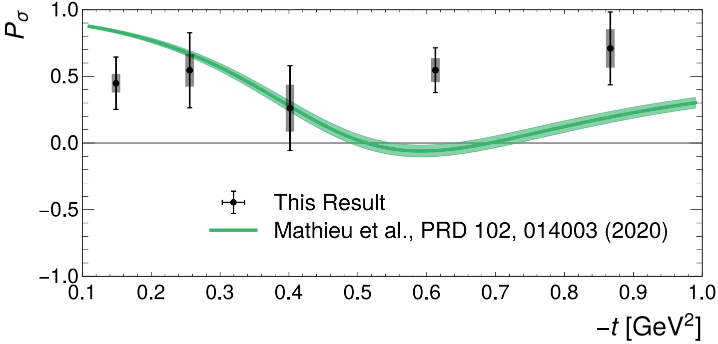

- We measure $P_\sigma \approx +0.5$, independent of t
- Significant deviation of TMD model from data for $-t \gtrsim 0.5\,(\mathrm{GeV}/c)^2$

Mathieu *et al.* [JPAC], PRD **102** (2020) 014003

Challenge: double-Regge contributions

Example: $\gamma\ p \to \eta\pi^0\ p$

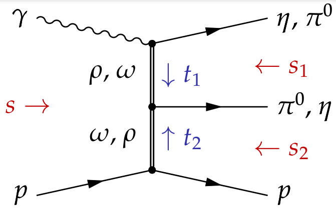

- Dominant at large $\eta\pi^0$ mass and low $|t_2|$
- Extend down to low-mass region and create background for resonances
- Important to understand and model
  - Can enhance spin-exotic odd-ℓ waves
  - Will interfere with resonances
  - Broad resonances such as $\pi_1(1600)$ may be masked, if not taken into account
- Theory support indispensible

Challenge: double-Regge contributions

Example: $\gamma\ p \to \eta\pi^0\ p$

- Dominant at large $\eta\pi^0$ mass and low $|t_2|$
- Extend down to low-mass region and create background for resonances
- Important to understand and model
  - Can enhance spin-exotic odd-ℓ waves
  - Will interfere with resonances
  - Broad resonances such as $\pi_1(1600)$ may be masked, if not taken into account
- Theory support indispensible

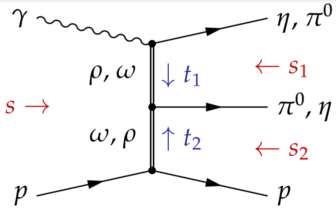

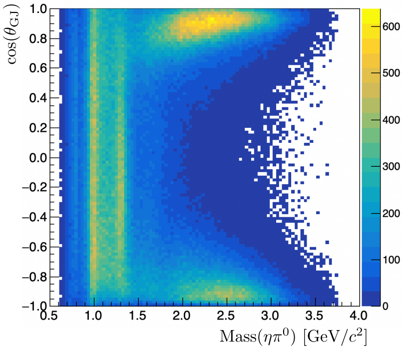

Challenge: double-Regge contributions

Example: $\gamma\ p \to \eta\pi^0\ p$

- Dominant at large $\eta\pi^0$ mass and low $|t_2|$
- Extend down to low-mass region and create background for resonances
- Important to understand and model
  - Can enhance spin-exotic odd-ℓ waves
  - Will interfere with resonances
  - Broad resonances such as $\pi_1(1600)$ may be masked, if not taken into account
- Theory support indispensible

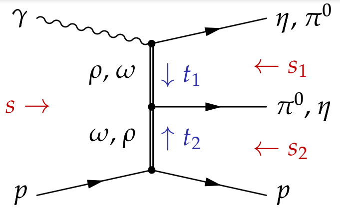

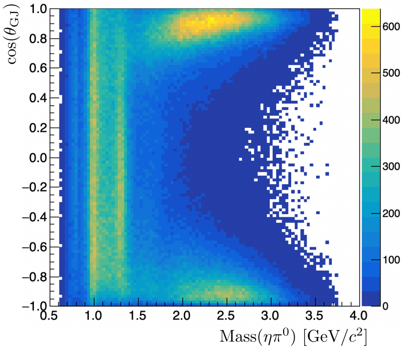

Modeling double-Regge processes

Example: $\gamma\, p \to \eta\pi^0\, p$

- Close collaboration with JPAC
  - Model describes distribution in all phase-space variables
  - Based on Bibrzycki *et al.* [JPAC], EPJC **81** (2021) 647
  - Improved description of vertex factors
  - Fit regions with fast η and fast π^0 separately
  - Reasonable agreement with data for $m_{\eta\pi} > 2\,\text{GeV}$
- Can we extrapolate model down to resonance region?

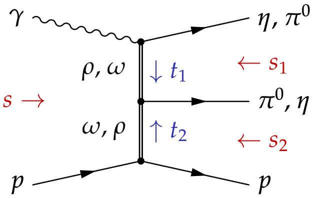

Modeling double-Regge processes

Example: $\gamma\, p \to \eta\pi^0\, p$

- Close collaboration with JPAC
  - Model describes distribution in all phase-space variables
  - Based on Bibrzycki *et al.* [JPAC], EPJC **81** (2021) 647
  - Improved description of vertex factors
  - Fit regions with fast η and fast π^0 separately
  - Reasonable agreement with data for $m_{\eta\pi} > 2\,\text{GeV}$
- Can we extrapolate model down to resonance region?

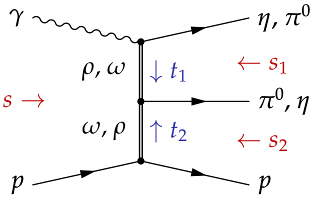

GlueX Internal

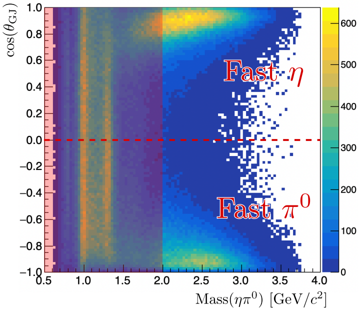

Modeling double-Regge processes

Example: $\gamma\, p \to \eta\pi^0\, p$

- Close collaboration with JPAC
  - Model describes distribution in all phase-space variables
  - Based on Bibrzycki *et al.* [JPAC], EPJC **81** (2021) 647
  - Improved description of vertex factors
  - Fit regions with fast η and fast π^0 separately
  - Reasonable agreement with data for $m_{\eta\pi} > 2\,\text{GeV}$
- Can we extrapolate model down to resonance region?

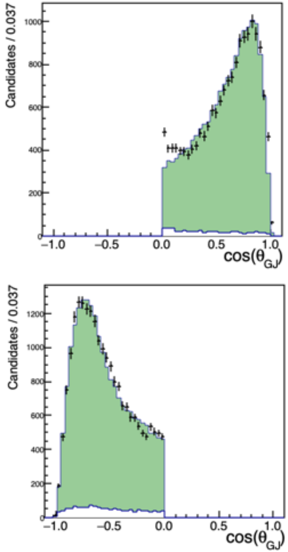

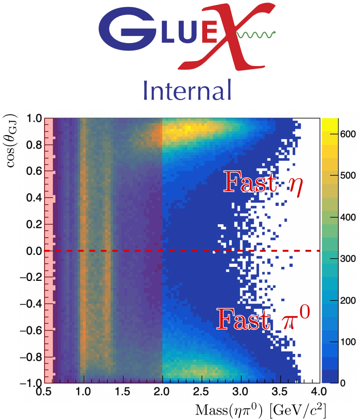

Modeling double-Regge processes

Example: $\gamma\, p \to \eta\pi^0\, p$

- Close collaboration with JPAC
  - Model describes distribution in all phase-space variables
  - Based on Bibrzycki *et al.* [JPAC], EPJC **81** (2021) 647
  - Improved description of vertex factors
  - Fit regions with fast η and fast π^0 separately
  - Reasonable agreement with data for $m_{\eta\pi} > 2\,\text{GeV}$
- Can we extrapolate model down to resonance region?

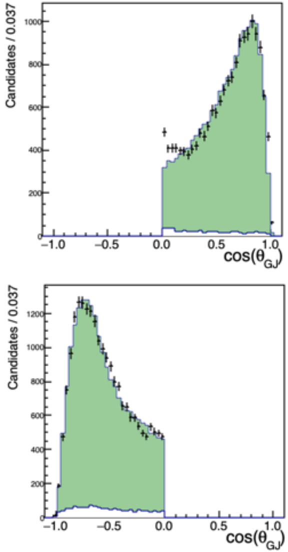

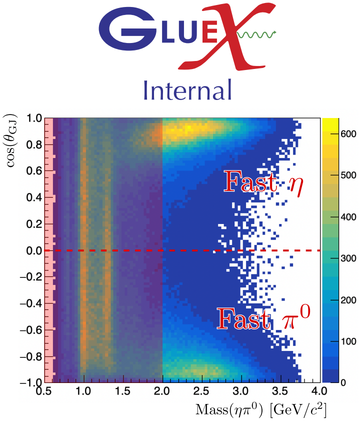

Additional challenge: baryon production

Example: $\gamma\ p \to \eta\pi^0\ p$

Meson production

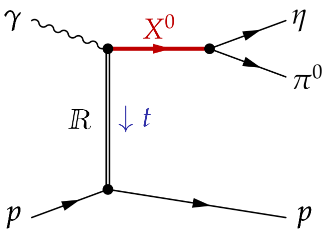

Double-Regge

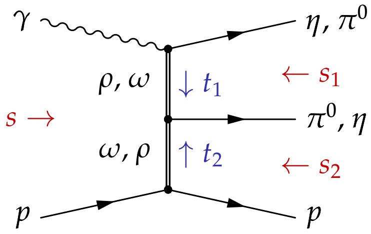

Baryon production

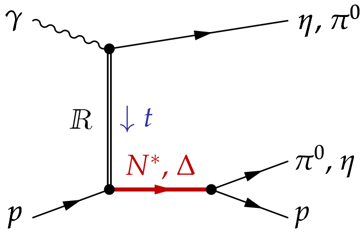

- Baryon production is dominant at high $\eta\pi$ mass
- Can by suppressed by removing low $\pi^0 p$ masses for fast η and low ηp masses for fast π^0
  - Cut strongly distorts angular acceptance
  - Irreducible backgrounds from higher baryon excitations remain

Moment analysis of two-body final states

Unpolarized case

Moment decomposition of angular distribution in $\Omega = (\theta, \phi)$

$$\mathcal{I}(\Omega) = \sum_{LM}^{\infty} \sqrt{\frac{2L+1}{4\pi}}\, H(L, M)\, Y_L^M(\Omega)$$

with

$$H(L, M) = \sqrt{\frac{4\pi}{2L+1}} \int_{4\pi} \mathrm{d}\Omega\, \mathcal{I}(\Omega)\, Y_L^{M*}(\Omega)$$

Advantages

- Moment decomposition is unique
- Does not assume a model $\Longrightarrow$ good way to pass experimental data to theorists

Disadvantages

- No direct access to partial-wave amplitudes
  - Would need to solve (overdetermined) second-order polynomial equation system

Moment decomposition of angular distribution in $\Omega = (\theta, \phi)$

$$\mathcal{I}(\Omega) = \sum_{LM}^{\infty} \sqrt{\frac{2L+1}{4\pi}}\, H(L, M)\, Y_L^M(\Omega)$$

with

$$H(L, M) = \sqrt{\frac{4\pi}{2L+1}} \int_{4\pi} \mathrm{d}\Omega\, \mathcal{I}(\Omega)\, Y_L^{M*}(\Omega)$$

Advantages

- Moment decomposition is unique
- Does not assume a model $\Longrightarrow$ good way to pass experimental data to theorists

Disadvantages

- No direct access to partial-wave amplitudes
  - Would need to solve (overdetermined) second-order polynomial equation system

Moment analysis of two-body final states

Unpolarized case

Moment decomposition of angular distribution in $\Omega = (\theta, \phi)$

$$\mathcal{I}(\Omega) = \sum_{LM}^{\infty} \sqrt{\frac{2L+1}{4\pi}}\, H(L, M)\, Y_L^M(\Omega)$$

with

$$H(L, M) = \sqrt{\frac{4\pi}{2L+1}} \int_{4\pi} \mathrm{d}\Omega\, \mathcal{I}(\Omega)\, Y_L^{M*}(\Omega)$$

Advantages

- Moment decomposition is unique
- Does not assume a model $\Longrightarrow$ good way to pass experimental data to theorists

Disadvantages

- No direct access to partial-wave amplitudes
  - Would need to solve (overdetermined) second-order polynomial equation system

- Measured intensity given by detector acceptance $\eta(\Omega)$: $\mathcal{I}_{\text{meas}}(\Omega) = \eta(\Omega)\,\mathcal{I}(\Omega)$
- Moment decomposition of $\mathcal{I}_{\text{meas}} \Longrightarrow$ measured moments

$$H_{\text{meas}}(L, M) = \sqrt{\frac{4\pi}{2L+1}} \int_{4\pi} \mathrm{d}\Omega\, \eta(\Omega)\, \mathcal{I}(\Omega)\, Y_L^{M*}(\Omega)$$

- Relate to physical moments $H(L', M')$ by inserting moment decomposition of physical intensity:

$$\mathcal{I}(\Omega) = \sum_{L'\,M'}^{\infty} \sqrt{\frac{2L'+1}{4\pi}}\, H(L', M')\, Y_{L'}^{M'}(\Omega)$$

- Acceptance mixes physical moments: $H_{\text{meas}}(L, M)$ are linear combinations of $H(L', M')$
- Matrix formulation: $\mathbf{H}_{\text{meas}} = \mathbf{I}_{\text{acc}}\, \mathbf{H} \quad \Longrightarrow \quad$ **physical moments:** $\mathbf{H} = (\mathbf{I}_{\text{acc}})^{-1}\, \mathbf{H}_{\text{meas}}$
- Acceptance integral matrix $\mathbf{I}_{\text{acc}}$ estimated using accepted phase-space events
- Estimate $\mathbf{H}_{\text{meas}}$ from data by replacing integral by sum over N_{meas} measured events with weights $\{w_i\}$

$$H_{\text{meas}}(L, M) = \sqrt{\frac{4\pi}{2L+1}} \sum_{k=1}^{N_{\text{meas}}} w_k\, Y_L^{M*}(\Omega_k)$$

with $\displaystyle\sum_{k=1}^{N_{\text{meas}}} w_k =$ number of events after background subtraction

- Measured intensity given by detector acceptance $\eta(\Omega)$: $\mathcal{I}_{\text{meas}}(\Omega) = \eta(\Omega)\,\mathcal{I}(\Omega)$
- Moment decomposition of $\mathcal{I}_{\text{meas}} \Longrightarrow$ measured moments

$$H_{\text{meas}}(L, M) = \sqrt{\frac{4\pi}{2L+1}} \int_{4\pi} \mathrm{d}\Omega\, \eta(\Omega)\, \mathcal{I}(\Omega)\, Y_L^{M*}(\Omega)$$

- Relate to physical moments $H(L', M')$ by inserting moment decomposition of physical intensity:

$$\mathcal{I}(\Omega) = \sum_{L'\,M'}^{\infty} \sqrt{\frac{2L'+1}{4\pi}}\, H(L', M')\, Y_{L'}^{M'}(\Omega)$$

- Acceptance mixes physical moments: $H_{\text{meas}}(L, M)$ are linear combinations of $H(L', M')$
- Matrix formulation: $\mathbf{H}_{\text{meas}} = \mathbf{I}_{\text{acc}}\,\mathbf{H} \quad\Longrightarrow\quad$ **physical moments:** $\mathbf{H} = (\mathbf{I}_{\text{acc}})^{-1}\,\mathbf{H}_{\text{meas}}$
- Acceptance integral matrix $\mathbf{I}_{\text{acc}}$ estimated using accepted phase-space events
- Estimate $\mathbf{H}_{\text{meas}}$ from data by replacing integral by sum over N_{meas} measured events with weights $\{w_i\}$

$$H_{\text{meas}}(L, M) = \sqrt{\frac{4\pi}{2L+1}} \sum_{k=1}^{N_{\text{meas}}} w_k\, Y_L^{M*}(\Omega_k)$$

with $\sum_{k=1}^{N_{\text{meas}}} w_k =$ number of events after background subtraction

- Measured intensity given by detector acceptance $\eta(\Omega)$: $\mathcal{I}_{\text{meas}}(\Omega) = \eta(\Omega)\,\mathcal{I}(\Omega)$
- Moment decomposition of $\mathcal{I}_{\text{meas}} \Longrightarrow$ measured moments

$$H_{\text{meas}}(L, M) = \sqrt{\frac{4\pi}{2L+1}} \int_{4\pi} \mathrm{d}\Omega\, \eta(\Omega)\, \mathcal{I}(\Omega)\, Y_L^{M*}(\Omega)$$

- Relate to physical moments $H(L', M')$ by inserting moment decomposition of physical intensity:

$$\mathcal{I}(\Omega) = \sum_{L'\,M'}^{\infty} \sqrt{\frac{2L'+1}{4\pi}}\, H(L', M')\, Y_{L'}^{M'}(\Omega)$$

- Acceptance mixes physical moments: $H_{\text{meas}}(L, M)$ are linear combinations of $H(L', M')$
- Matrix formulation: $\mathbf{H}_{\text{meas}} = \mathbf{I}_{\text{acc}}\,\mathbf{H} \quad \Longrightarrow \quad$ **physical moments:** $\mathbf{H} = (\mathbf{I}_{\text{acc}})^{-1}\,\mathbf{H}_{\text{meas}}$
- Acceptance integral matrix $\mathbf{I}_{\text{acc}}$ estimated using accepted phase-space events
- Estimate $\mathbf{H}_{\text{meas}}$ from data by replacing integral by sum over N_{meas} measured events with weights $\{w_i\}$

$$H_{\text{meas}}(L, M) = \sqrt{\frac{4\pi}{2L+1}} \sum_{k=1}^{N_{\text{meas}}} w_k\, Y_L^{M*}(\Omega_k)$$

with $\sum_{k=1}^{N_{\text{meas}}} w_k =$ number of events after background subtraction

Moment analysis of two-body final states

Correcting for acceptance effects

- Measured intensity given by detector acceptance $\eta(\Omega)$: $\mathcal{I}_{\text{meas}}(\Omega) = \eta(\Omega)\,\mathcal{I}(\Omega)$
- Moment decomposition of $\mathcal{I}_{\text{meas}} \Longrightarrow$ measured moments

$$H_{\text{meas}}(L, M) = \sqrt{\frac{4\pi}{2L+1}} \int_{4\pi} \mathrm{d}\Omega\, \eta(\Omega)\, \mathcal{I}(\Omega)\, Y_L^{M*}(\Omega)$$

- Relate to physical moments $H(L', M')$ by inserting moment decomposition of physical intensity:

$$\mathcal{I}(\Omega) = \sum_{L'\,M'}^{\infty} \sqrt{\frac{2L'+1}{4\pi}}\, H(L', M')\, Y_{L'}^{M'}(\Omega)$$

- Acceptance mixes physical moments: $H_{\text{meas}}(L, M)$ are linear combinations of $H(L', M')$
- Matrix formulation: $\mathbf{H}_{\text{meas}} = \mathbf{I}_{\text{acc}}\,\mathbf{H} \quad \Longrightarrow$ **physical moments:** $\mathbf{H} = (\mathbf{I}_{\text{acc}})^{-1}\,\mathbf{H}_{\text{meas}}$
- Acceptance integral matrix $\mathbf{I}_{\text{acc}}$ estimated using accepted phase-space events
- Estimate $\mathbf{H}_{\text{meas}}$ from data by replacing integral by sum over N_{meas} measured events with weights $\{w_i\}$

$$H_{\text{meas}}(L, M) = \sqrt{\frac{4\pi}{2L+1}} \sum_{k=1}^{N_{\text{meas}}} w_k\, Y_L^{M*}(\Omega_k)$$

with $\sum_{k=1}^{N_{\text{meas}}} w_k =$ number of events after background subtraction

Moment analysis of two-body final states

Correcting for acceptance effects

- Measured intensity given by detector acceptance $\eta(\Omega)$: $\mathcal{I}_{\text{meas}}(\Omega) = \eta(\Omega)\,\mathcal{I}(\Omega)$
- Moment decomposition of $\mathcal{I}_{\text{meas}} \Longrightarrow$ measured moments

$$H_{\text{meas}}(L, M) = \sqrt{\frac{4\pi}{2L+1}} \int_{4\pi} \mathrm{d}\Omega\, \eta(\Omega)\, \mathcal{I}(\Omega)\, Y_L^{M*}(\Omega)$$

- Relate to physical moments $H(L', M')$ by inserting moment decomposition of physical intensity:

$$\mathcal{I}(\Omega) = \sum_{L'\,M'}^{\infty} \sqrt{\frac{2L'+1}{4\pi}}\, H(L', M')\, Y_{L'}^{M'}(\Omega)$$

- Acceptance mixes physical moments: $H_{\text{meas}}(L, M)$ are linear combinations of $H(L', M')$
- Matrix formulation: $\mathbf{H}_{\text{meas}} = \mathbf{I}_{\text{acc}}\,\mathbf{H} \quad \Longrightarrow \quad$ **physical moments:** $\mathbf{H} = (\mathbf{I}_{\text{acc}})^{-1}\,\mathbf{H}_{\text{meas}}$
- Acceptance integral matrix $\mathbf{I}_{\text{acc}}$ estimated using accepted phase-space events
- Estimate $\mathbf{H}_{\text{meas}}$ from data by replacing integral by sum over N_{meas} measured events with weights $\{w_i\}$

$$H_{\text{meas}}(L, M) = \sqrt{\frac{4\pi}{2L+1}} \sum_{k=1}^{N_{\text{meas}}} w_k\, Y_L^{M*}(\Omega_k)$$

with $\sum_{k=1}^{N_{\text{meas}}} w_k =$ number of events after background subtraction

Moment analysis of two-body final states

Correcting for acceptance effects

- Measured intensity given by detector acceptance $\eta(\Omega)$: $\mathcal{I}_{\text{meas}}(\Omega) = \eta(\Omega)\,\mathcal{I}(\Omega)$
- Moment decomposition of $\mathcal{I}_{\text{meas}} \Longrightarrow$ measured moments

$$H_{\text{meas}}(L, M) = \sqrt{\frac{4\pi}{2L+1}} \int_{4\pi} \mathrm{d}\Omega\, \eta(\Omega)\, \mathcal{I}(\Omega)\, Y_L^{M*}(\Omega)$$

- Relate to physical moments $H(L', M')$ by inserting moment decomposition of physical intensity:

$$\mathcal{I}(\Omega) = \sum_{L'\,M'}^{\infty} \sqrt{\frac{2L'+1}{4\pi}}\, H(L', M')\, Y_{L'}^{M'}(\Omega)$$

- Acceptance mixes physical moments: $H_{\text{meas}}(L, M)$ are linear combinations of $H(L', M')$
- Matrix formulation: $\mathbf{H}_{\text{meas}} = \mathbf{I}_{\text{acc}}\,\mathbf{H} \quad \Longrightarrow \quad$ **physical moments:** $\mathbf{H} = (\mathbf{I}_{\text{acc}})^{-1}\,\mathbf{H}_{\text{meas}}$
- Acceptance integral matrix $\mathbf{I}_{\text{acc}}$ estimated using accepted phase-space events
- Estimate $\mathbf{H}_{\text{meas}}$ from data by replacing integral by sum over N_{meas} measured events with weights $\{w_i\}$

$$H_{\text{meas}}(L, M) = \sqrt{\frac{4\pi}{2L+1}} \sum_{k=1}^{N_{\text{meas}}} w_k\, Y_L^{M*}(\Omega_k)$$

with $\displaystyle\sum_{k=1}^{N_{\text{meas}}} w_k =$ number of events after background subtraction

Moment analysis of unpolarized $\gamma\, p \to \pi^+\pi^-\, p$

CLAS Results for $3.6 < E_\gamma < 3.8$ GeV

Jefferson Lab
Thomas Jefferson National Accelerator Facility

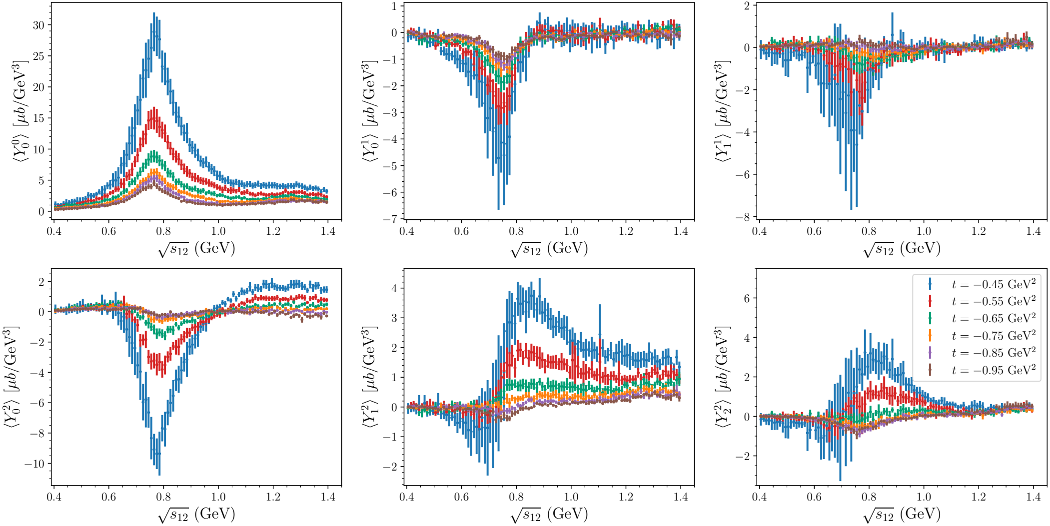

$\sqrt{s_{12}} = m_{\pi\pi}$

Battaglieri *et al.* [CLAS], PRD **80** (2009) 072005; Fig. from Bibrzycki *et al.* [JPAC], PRD **111** (2025) 014002

JPAC analysis of $\pi^+\pi^-$ moments from CLAS

Bibrzycki *et al.* [JPAC], PRD **111** (2025) 014002 CLAS, PRD **80** (2009) 072005

Jefferson Lab
Thomas Jefferson National Accelerator Facility

- JPAC: fit of lowest 6 moments in highest energy bin $3.6 < E_\gamma < 3.8\,\text{GeV}$ from CLAS analysis
- Model: resonances $f_0(500)$, $\rho(770)$, $f_0(980)$, $f_2(1270)$, $f_0(1370)$ + Deck process + non-resonant polynomial in $s_{12} = m^2_{\pi\pi}$
- Resonance production modeled using Regge trajectories: ρ and ω for $J^P = 0^+$ and 2^+; $\mathbb{P}$, a_2, and f_2 for $J^P = 1^-$

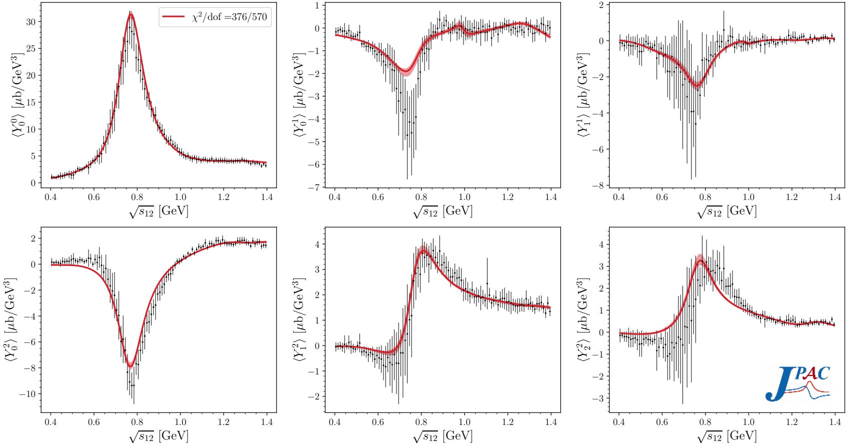

- Resonances described using Breit-Wigner amplitudes
- Resonance parameters fixed
- 30 free parameters: relative strengths and phases of production mechanisms for each model component
- Each t bin fitted independently

$0.4 < |t| < 0.5\,\text{GeV}^2$

JPAC analysis of $\pi^+\pi^-$ moments from CLAS

Bibrzycki *et al.* [JPAC], PRD **111** (2025) 014002 CLAS, PRD **80** (2009) 072005

- JPAC: fit of lowest 6 moments in highest energy bin $3.6 < E_\gamma < 3.8\,\text{GeV}$ from CLAS analysis
- Model: resonances $f_0(500)$, $\rho(770)$, $f_0(980)$, $f_2(1270)$, $f_0(1370)$ + Deck process + non-resonant polynomial in $s_{12} = m^2_{\pi\pi}$
- Resonance production modeled using Regge trajectories: ρ and ω for $J^P = 0^+$ and 2^+; $\mathbb{P}$, a_2, and f_2 for $J^P = 1^-$

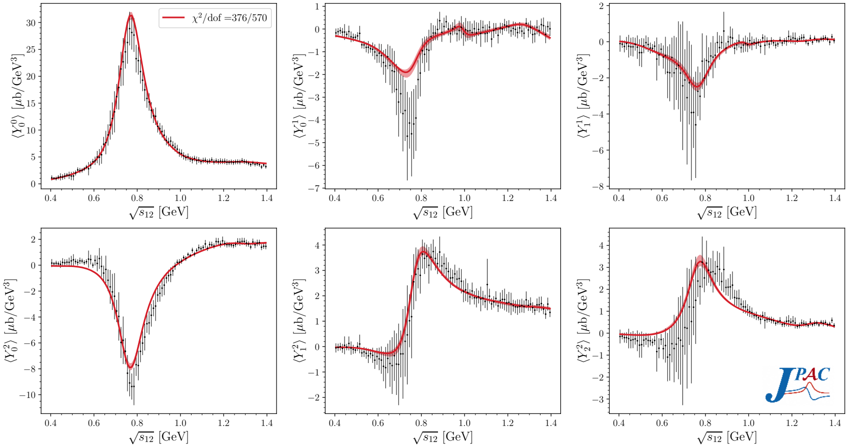

- Resonances described using Breit-Wigner amplitudes
- Resonance parameters fixed
- 30 free parameters: relative strengths and phases of production mechanisms for each model component
- Each t bin fitted independently

$0.4 < |t| < 0.5\,\text{GeV}^2$

JPAC analysis of $\pi^+\pi^-$ moments from CLAS

Bibrzycki *et al.* [JPAC], PRD **111** (2025) 014002 CLAS, PRD **80** (2009) 072005

- JPAC: fit of lowest 6 moments in highest energy bin $3.6 < E_\gamma < 3.8$ GeV from CLAS analysis
- Model: resonances $f_0(500)$, $\rho(770)$, $f_0(980)$, $f_2(1270)$, $f_0(1370)$ + Deck process + non-resonant polynomial in $s_{12} = m^2_{\pi\pi}$
- Resonance production modeled using Regge trajectories: ρ and ω for $J^P = 0^+$ and 2^+; $\mathbb{P}$, a_2, and f_2 for $J^P = 1^-$

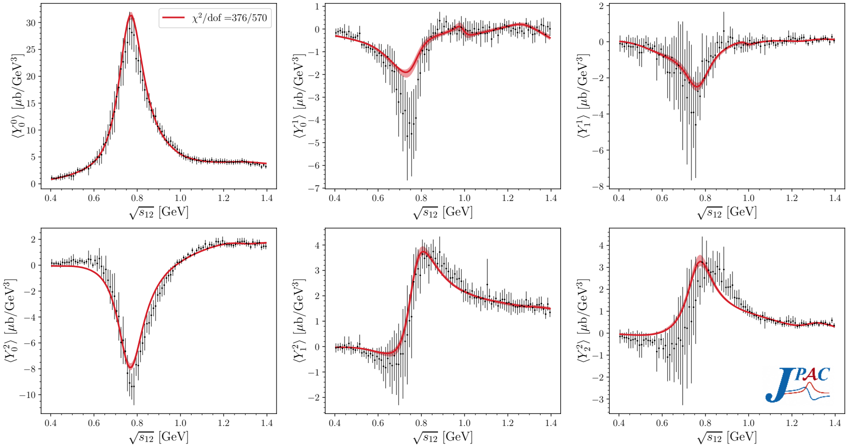

- Resonances described using Breit-Wigner amplitudes
- Resonance parameters fixed
- 30 free parameters: relative strengths and phases of production mechanisms for each model component
- Each t bin fitted independently

$0.4 < |t| < 0.5\,\text{GeV}^2$

JPAC analysis of $\pi^+\pi^-$ moments from CLAS

Bibrzycki *et al.* [JPAC], PRD **111** (2025) 014002   CLAS, PRD **80** (2009) 072005

Jefferson Lab
Thomas Jefferson National Accelerator Facility

- JPAC: fit of lowest 6 moments in highest energy bin $3.6 < E_\gamma < 3.8$ GeV from CLAS analysis
- Model: resonances $f_0(500)$, $\rho(770)$, $f_0(980)$, $f_2(1270)$, $f_0(1370)$ + Deck process + non-resonant polynomial in $s_{12} = m^2_{\pi\pi}$
- Resonance production modeled using Regge trajectories: ρ and ω for $J^P = 0^+$ and 2^+; $\mathbb{P}$, a_2, and f_2 for $J^P = 1^-$

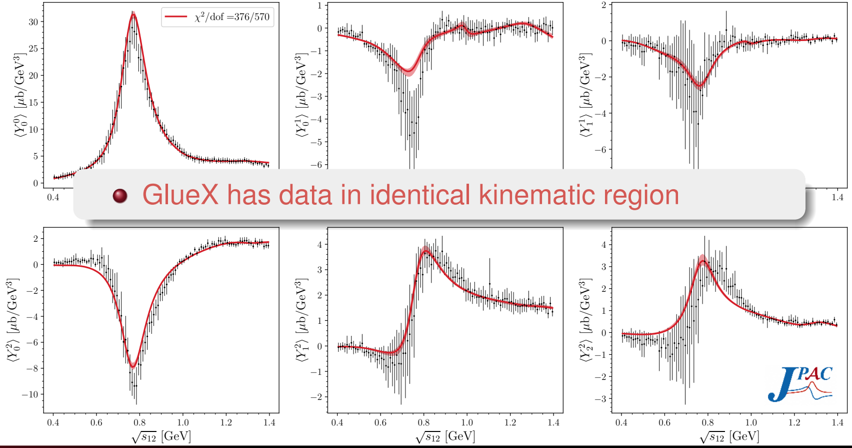

- GlueX has data in identical kinematic region

- Resonances described using Breit-Wigner amplitudes
- Resonance parameters fixed
- 30 free parameters: relative strengths and phases of production mechanisms for each model component
- Each t bin fitted independently

$0.4 < |t| < 0.5$ GeV^2

- $H(0,0) = \sqrt{4\pi} \int_{4\pi} \mathrm{d}\Omega\, \mathcal{I}(\Omega)\, \underbrace{Y_0^{0*}(\Omega)}_{=1/\sqrt{4\pi}} = \int_{4\pi} \mathrm{d}\Omega\, \mathcal{I}(\Omega) =$ number of acceptance-corrected events

- All CLAS and JPAC moments scaled by same factor such that $\int \mathrm{d}m_{\pi\pi}\, H_{\text{CLAS}}(0,0) = \int \mathrm{d}m_{\pi\pi}\, H_{\text{GlueX}}(0,0)$
- Error bars of CLAS points dominanted by systematic uncertainties
- Only statistical uncertainties for GlueX
- Good qualitative agreement of GlueX results with CLAS/JPAC

- $H(0,0) = \sqrt{4\pi}\int_{4\pi} \mathrm{d}\Omega\,\mathcal{I}(\Omega)\,\underbrace{Y_0^{0*}(\Omega)}_{=1/\sqrt{4\pi}} = \int_{4\pi}\mathrm{d}\Omega\,\mathcal{I}(\Omega) =$ number of acceptance-corrected events

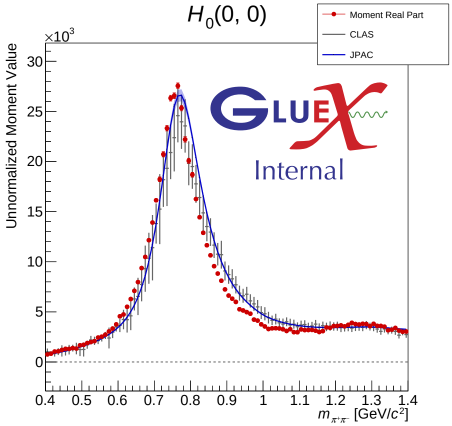

- All CLAS and JPAC moments scaled by same factor such that $\int \mathrm{d}m_{\pi\pi}\, H_{\text{CLAS}}(0,0) = \int \mathrm{d}m_{\pi\pi}\, H_{\text{GlueX}}(0,0)$
- Error bars of CLAS points dominanted by systematic uncertainties
- Only statistical uncertainties for GlueX
- Good qualitative agreement of GlueX results with CLAS/JPAC

Moment analysis of unpolarized $\gamma\, p \to \pi^+\pi^-\, p$

Example Results

$H(2,0) = \ldots\ -|P_{-1}|^2 + 2|P_0|^2\ -|P_{+1}|^2 \ldots$

$H(2,1) = \mathrm{Re}\left[\ldots - P^*_{-1}\, P_0 - P^*_{+1}\, P_0 \ldots\right]$

$H(2,2) = \mathrm{Re}\left[\ldots - P^*_{-1}\, P_{+1} \ldots\right]$

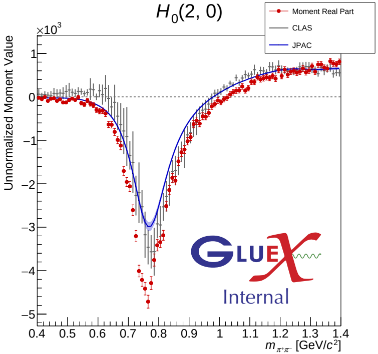

- P_0 wave smaller than $P_{\pm 1}$ waves; P_0 and $P_{\pm 1}$ amplitudes not phase locked
- GlueX results agree qualitatively with CLAS/JPAC; deviations in details

Moment analysis of unpolarized $\gamma\, p \to \pi^+\pi^-\, p$

Example Results

$H(2,0) = \ldots -|P_{-1}|^2 + 2|P_0|^2 - |P_{+1}|^2 \ldots$

$H(2,1) = \mathrm{Re}\left[\ldots - P^*_{-1}\, P_0 - P^*_{+1}\, P_0 \ldots\right]$

$H(2,2) = \mathrm{Re}\left[\ldots - P^*_{-1}\, P_{+1} \ldots\right]$

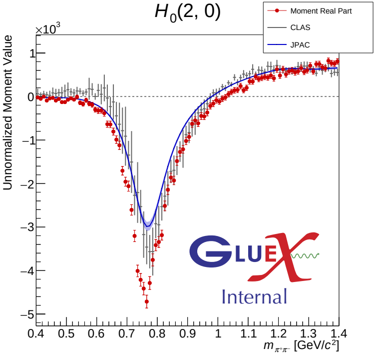

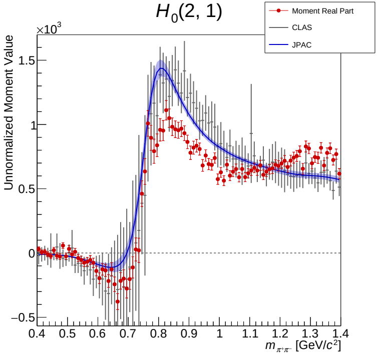

- P_0 wave smaller than $P_{\pm 1}$ waves; P_0 and $P_{\pm 1}$ amplitudes not phase locked
- GlueX results agree qualitatively with CLAS/JPAC; deviations in details

Moment analysis of unpolarized $\gamma\, p \to \pi^+\pi^-\, p$

Example Results

Jefferson Lab
Thomas Jefferson National Accelerator Facility

$$H(2,0) = \ldots - |P_{-1}|^2 + 2|P_0|^2 - |P_{+1}|^2 \ldots$$

$$H(2,1) = \mathrm{Re}\left[\ldots - P^*_{-1}\, P_0 - P^*_{+1}\, P_0 \ldots\right]$$

$$H(2,2) = \mathrm{Re}\left[\ldots - P^*_{-1}\, P_{+1} \ldots\right]$$

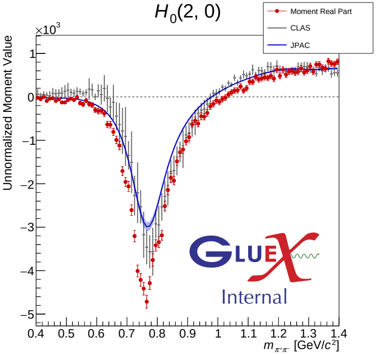

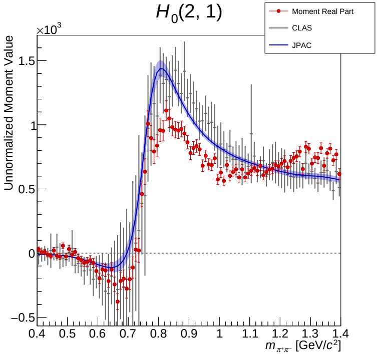

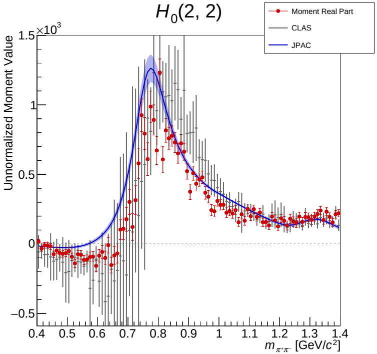

- P_0 wave smaller than $P_{\pm 1}$ waves; P_0 and $P_{\pm 1}$ amplitudes not phase locked
- GlueX results agree qualitatively with CLAS/JPAC; deviations in details

Moment analysis of $\gamma\, p \to \pi^+\pi^-\, p$

Jefferson Lab
Thomas Jefferson National Accelerator Facility

Work in progress

- Use GlueX data to extend $\pi^+\pi^-$ moment analysis to
  - Linearly polarized photon beams
  - Higher beam energies
  - Lower momentum transfers
  - Higher $\pi^+\pi^-$ masses
  - Higher precision

Opportunity: moment analyses are good testing grounds for

- Surrogate models of detector acceptance
- Parameter estimation methods
  - Moment decomposition of intensity is unique
  - But moment values may lead to unphysical, i.e. negative intensities

Moment analysis of $\gamma\, p \to \pi^+\pi^-\, p$

Jefferson Lab
Thomas Jefferson National Accelerator Facility

Work in progress

- Use GlueX data to extend $\pi^+\pi^-$ moment analysis to
  - Linearly polarized photon beams
  - Higher beam energies
  - Lower momentum transfers
  - Higher $\pi^+\pi^-$ masses
  - Higher precision

Opportunity: moment analyses are good testing grounds for

- Surrogate models of detector acceptance
- Parameter estimation methods
  - Moment decomposition of intensity is unique
  - But moment values may lead to unphysical, i.e. negative intensities

Conclusions

Jefferson Lab
Thomas Jefferson National Accelerator Facility

Challenges in amplitude analyses provide opportunities for AI applications

- Accelerating computations by replacing expensive functions with surrogate models, e.g. for detector acceptance, would
  - allow exploration of larger model spaces
  - make advanced methods such as Markov chain Monte Carlo more feasible
  - allow more detailed input-output studies
  - ...
- Model selection
  - Determination of optimal wave sets
  - Determination of minimal resonance content
- Imposing continuity and smoothness constraints on amplitudes
- Alternative approaches for parameter estimation
- ...

Conclusions

Jefferson Lab
Thomas Jefferson National Accelerator Facility

Challenges in amplitude analyses provide opportunities for AI applications

- Accelerating computations by replacing expensive functions with surrogate models, e.g. for detector acceptance, would
  - allow exploration of larger model spaces
  - make advanced methods such as Markov chain Monte Carlo more feasible
  - allow more detailed input-output studies
  - ...
- Model selection
  - Determination of optimal wave sets
  - Determination of minimal resonance content
- Imposing continuity and smoothness constraints on amplitudes
- Alternative approaches for parameter estimation
- ...

Conclusions

Jefferson Lab
Thomas Jefferson National Accelerator Facility

Challenges in amplitude analyses provide opportunities for AI applications

- Accelerating computations by replacing expensive functions with surrogate models, e.g. for detector acceptance, would
  - allow exploration of larger model spaces
  - make advanced methods such as Markov chain Monte Carlo more feasible
  - allow more detailed input-output studies
  - . . .
- Model selection
  - Determination of optimal wave sets
  - Determination of minimal resonance content
- Imposing continuity and smoothness constraints on amplitudes
- Alternative approaches for parameter estimation
- . . .

Part II

Backup Slides

Backup Slides

GlueX Data

↓

Pseudoscalar + Pseudoscalar
$\pi\pi$ / $K\bar{K}$ / $\pi\eta$ / $\pi\eta'$ / $\eta\eta'$

↓

Vector + Pseudoscalar
$\omega\pi$ / $\omega\eta$ / $\phi\pi$ / $\phi\eta$ / $\phi\omega$

↓

3-body f nal states
$\eta\pi\pi$ / $K\bar{K}\pi$ / …

Complexity ↓

Possible Exotic Hybrid Meson Decays

π_1: $\eta\pi$ / $\eta'\pi$, η_1: $\eta\eta'$

h_2,ω_0: $\omega\eta$, h_2',ϕ_0: $\phi\eta$
ρ_0: $\omega\pi$, $\phi\pi$

η_1,b_2: $\eta\pi\pi$, η_1',h_2': $KK\pi$

- *Strategy:* understand photoproduction of well-known states first and then use them as reference when searching for exotic states
- "Golden channels" for π_1 search: $\eta\pi$ and $\eta'\pi$ $\Longrightarrow$ focus of this talk

GlueX Data

↓

Pseudoscalar + Pseudoscalar
$\pi\pi$ / $K\bar{K}$ / $\pi\eta$ / $\pi\eta'$ / $\eta\eta'$

↓

Vector + Pseudoscalar
$\omega\pi$ / $\omega\eta$ / $\phi\pi$ / $\phi\eta$ / $\phi\omega$

↓

3-body f nal states
$\eta\pi\pi$ / $K\bar{K}\pi$ / …

Complexity

Possible Exotic Hybrid Meson Decays

π_1: $\eta\pi$ / $\eta'\pi$, η_1: $\eta\eta'$

h_2,ω_0: $\omega\eta$, h_2',ϕ_0: $\phi\eta$
ρ_0: $\omega\pi$, $\phi\pi$

η_1,b_2: $\eta\pi\pi$, η_1',h_2': $KK\pi$

- *Strategy:* understand photoproduction of well-known states first and then use them as reference when searching for exotic states
- "Golden channels" for π_1 search: $\eta\pi$ and $\eta'\pi$ $\Longrightarrow$ focus of this talk

Searching for Exotics at GlueX

Possible Exotic Hybrid Meson Decays

GlueX Data

↓

Pseudoscalar + Pseudoscalar
$\pi\pi$ / $K\bar{K}$ / $\pi\eta$ / $\pi\eta'$ / $\eta\eta'$

π_1: $\eta\pi$ / $\eta'\pi$, η_1: $\eta\eta'$

↓

Vector + Pseudoscalar
$\omega\pi$ / $\omega\eta$ / $\phi\pi$ / $\phi\eta$ / $\phi\omega$

h_2,ω_0: $\omega\eta$, h_2',ϕ_0: $\phi\eta$
ρ_0: $\omega\pi$, $\phi\pi$

↓

3-body f nal states
$\eta\pi\pi$ / $K\bar{K}\pi$ / …

η_1,b_2: $\eta\pi\pi$, η_1',h_2': $KK\pi$

Complexity

- *Strategy:* understand photoproduction of well-known states first and then use them as reference when searching for exotic states
- "Golden channels" for π_1 search: $\eta\pi$ and $\eta'\pi$ $\Longrightarrow$ focus of this talk

Photoproduction

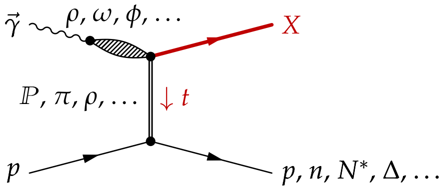

Exchange		Spin-exotic states	
$\mathbb{P}$	0^{++}	b, h, h'	$0^{+-}, 2^{+-}$
π^0	0^{-+}	b_2, h_2, h_2'	2^{+-}
$\pi^\pm$	0^{-+}	π_1	1^{-+}
ω	1^{--}	π_1, η_1, η_1'	1^{-+}

- Wide variety of intermediate states X accessible
- Photon polarization provides constraints on production process
- *Prerequisite:* understanding of production mechanism
- Existing photoproduction data very limited

Goal of GlueX

- Confirm π_1 and η_1
- Establish full light-quark hybrid spectrum

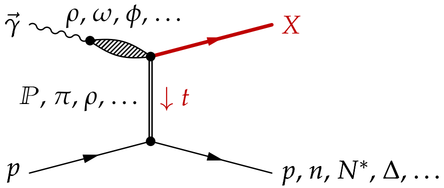

Exchange		Spin-exotic states	
$\mathbb{P}$	0^{++}	b, h, h'	$0^{+-}, 2^{+-}$
π^0	0^{-+}	b_2, h_2, h'_2	2^{+-}
$\pi^\pm$	0^{-+}	π_1	1^{-+}
ω	1^{--}	π_1, η_1, η'_1	1^{-+}

- Wide variety of intermediate states X accessible
- Photon polarization provides constraints on production process
- *Prerequisite:* understanding of production mechanism
- Existing photoproduction data very limited

Goal of GlueX

- Confirm π_1 and η_1
- Establish full light-quark hybrid spectrum

Photoproduction

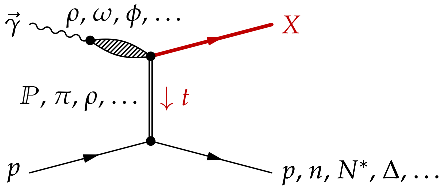

Exchange		Spin-exotic states	
$\mathbb{P}$	0^{++}	b, h, h'	$0^{+-}, 2^{+-}$
π^0	0^{-+}	b_2, h_2, h'_2	2^{+-}
$\pi^\pm$	0^{-+}	π_1	1^{-+}
ω	1^{--}	π_1, η_1, η'_1	1^{-+}

- Wide variety of intermediate states X accessible
- Photon polarization provides constraints on production process
- *Prerequisite:* understanding of production mechanism
- Existing photoproduction data very limited

Goal of GlueX

- Confirm π_1 and η_1
- Establish full light-quark hybrid spectrum

The GlueX Experiment at Jefferson Lab

Adhikari *et al.*, NIMA **987** (2021) 164807

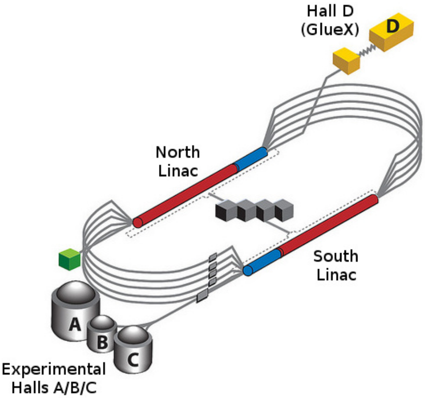

- 12 GeV e^- beam from CEBAF
- Diamond radiator $\Longrightarrow$ linearly polarized photon beam
- Photon energy tagged by scattered e^-; $\sigma(E_\gamma) = 0.2\,\%$
- Coherent peak: 1 to $5 \times 10^7\ \gamma/\mathrm{s}$ with $\approx 40\,\%$ polarization

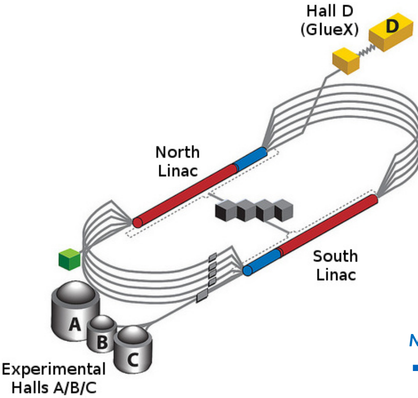

- 12 GeV e^- beam from CEBAF
- Diamond radiator $\Longrightarrow$ linearly polarized photon beam
- Photon energy tagged by scattered e^-; $\sigma(E_\gamma) = 0.2\,\%$
- Coherent peak: 1 to 5 × 10^7 γ/s with $\approx$ 40 % polarization

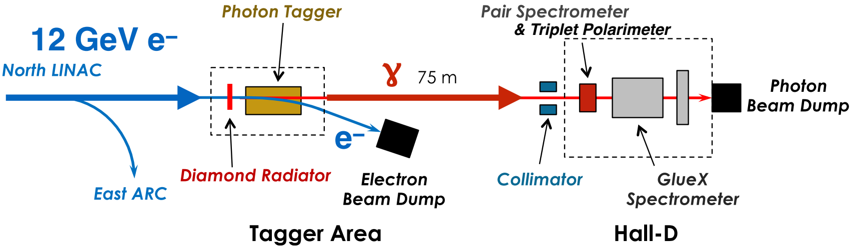

The GlueX Experiment at Jefferson Lab

Adhikari *et al.*, NIMA **987** (2021) 164807

Jefferson Lab
Thomas Jefferson National Accelerator Facility

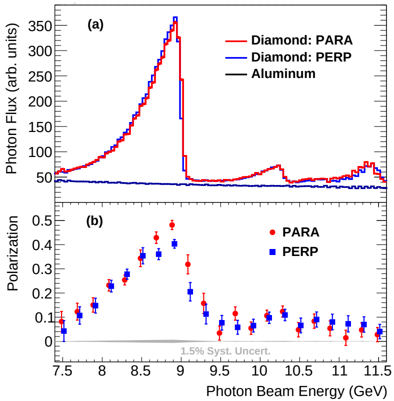

- 12 GeV e^- beam from CEBAF
- Diamond radiator $\Longrightarrow$ linearly polarized photon beam
- Photon energy tagged by scattered e^-; $\sigma(E_\gamma) = 0.2\,\%$
- Coherent peak: 1 to 5 × 10^7 γ/s with $\approx 40\,\%$ polarization

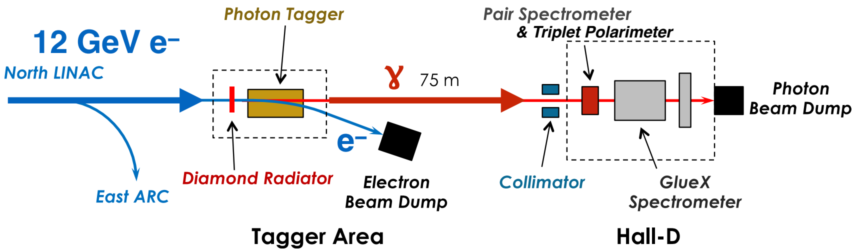

The GlueX Experiment at Jefferson Lab

Adhikari *et al.*, NIMA **987** (2021) 164807

Jefferson Lab
Thomas Jefferson National Accelerator Facility

- Large-acceptance spectrometer
- Optimized for light-meson spectroscopy
- **GlueX Phase I**
  - 2017 to 2018
  - $\int\mathcal{L} = 125\,\mathrm{pb}^{-1}$ in coherent peak
- **GlueX Phase II**
  - 2020 to 2025?
  - Added DIRC for PID
  - So far $\int\mathcal{L} = 190\,\mathrm{pb}^{-1}$ in coherent peak
  - Expect 3 to 4$\times$ Phase I

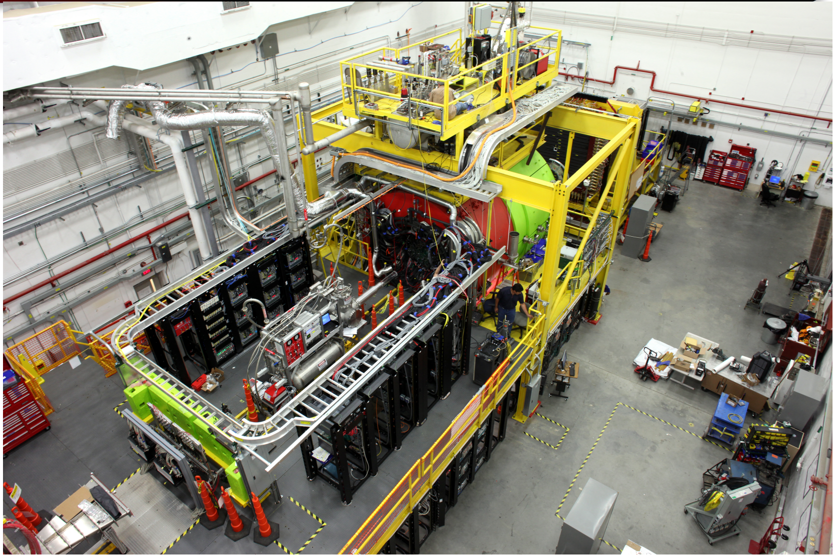

Adhikari *et al.*, NIMA **987** (2021) 164807

Jefferson Lab
Thomas Jefferson National Accelerator Facility

- Large-acceptance spectrometer
- Optimized for light-meson spectroscopy
- **GlueX Phase I**
  - 2017 to 2018
  - $\int \mathcal{L} = 125\,\mathrm{pb}^{-1}$ in coherent peak
- **GlueX Phase II**
  - 2020 to 2025?
  - Added DIRC for PID
  - So far $\int \mathcal{L} = 190\,\mathrm{pb}^{-1}$ in coherent peak
  - Expect 3 to 4× Phase I

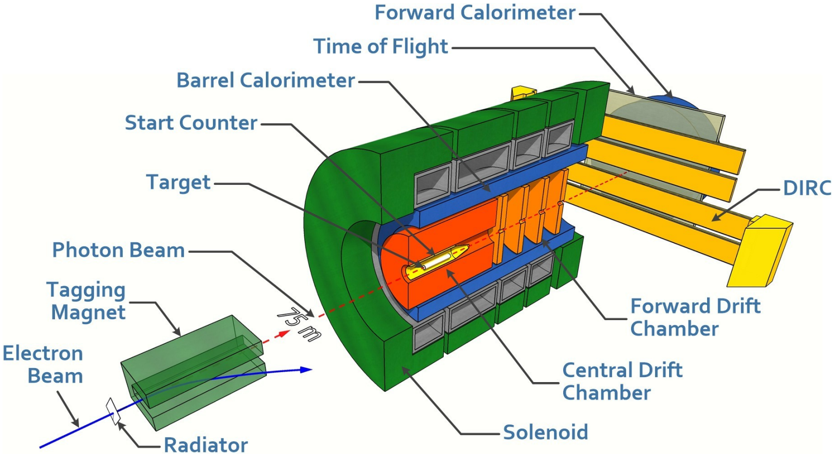

The GlueX Experiment at Jefferson Lab

Adhikari *et al.*, NIMA **987** (2021) 164807

Jefferson Lab
Thomas Jefferson National Accelerator Facility

- Large-acceptance spectrometer
- Optimized for light-meson spectroscopy
- **GlueX Phase I**
  - 2017 to 2018
  - $\int\mathcal{L} = 125\,\mathrm{pb}^{-1}$ in coherent peak
- **GlueX Phase II**
  - 2020 to 2025?
  - Added DIRC for PID
  - So far $\int\mathcal{L} = 190\,\mathrm{pb}^{-1}$ in coherent peak
  - Expect 3 to 4× Phase I

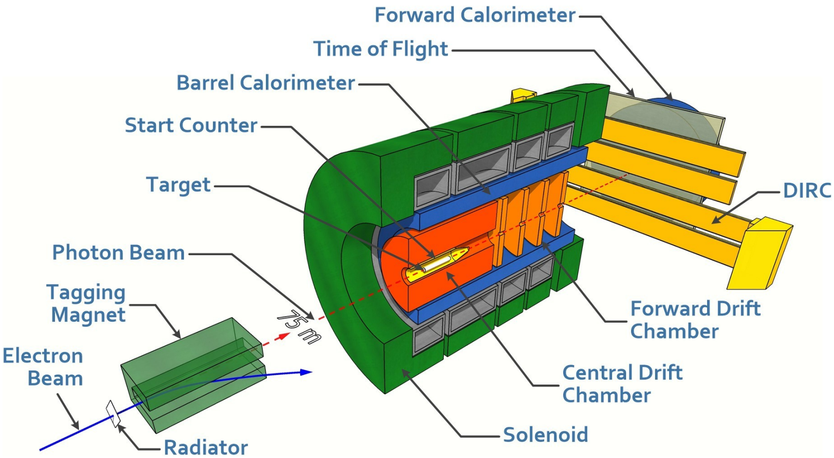

- Large-acceptance spectrometer
- Optimized for light-meson spectroscopy
- **GlueX Phase I**
  - 2017 to 2018
  - $\int\mathcal{L} = 125\,\mathrm{pb}^{-1}$ in coherent peak
- **GlueX Phase II**
  - 2020 to 2025?
  - Added DIRC for PID
  - So far $\int\mathcal{L} = 190\,\mathrm{pb}^{-1}$ in coherent peak
  - Expect 3 to 4$\times$ Phase I